PHYSICAL REVIEW B **69**, 041308(R) (2004)

Electron paramagnetic resonance study of $Zn_{1-x}Co_xO$: A predicted high-temperature ferromagnetic semiconductor

N. Jedrecy,[1,*] H. J. von Bardeleben,[2] Y. Zheng,[1] and J-L. Cantin[2]
[1]*Laboratoire de Minéralogie–Cristallographie, associé au CNRS et aux Universités Paris 6 et 7, Université de Paris VI, 4 place Jussieu, 75252 Paris Cedex 05, France*
[2]*Groupe de Physique des Solides, Associés au CNRS et aux Universités Paris 6 et Paris 7, 4 place Jussieu, 75005 Paris, France*
(Received 5 November 2003; published 29 January 2004)

The magnetic properties of Co^{2+} ions in epitaxial (Zn,Co)O layers with 10% Co concentration have been studied by electron paramagnetic resonance spectroscopy. The Co-related EPR spectrum is characterized by a 200-G broad anisotropic single line with g factors close to those of the isolated Co^{2+} ion. The temperature dependence of the EPR signal follows a Curie-Weiss law with a critical temperature of +12 K. We find no evidence for a high-temperature ferromagnetic state. Magnetocrystalline anisotropy is observed and a canted spin arrangement is suggested.

DOI: 10.1103/PhysRevB.69.041308 PACS number(s): 75.20.−g, 75.25.+z, 76.30.−v

Developments in spin-transport electronics depend in large part on the elaboration of ferromagnetic semiconductors with Curie temperatures above room temperature. The diluted magnetic semiconductors (DMS's) in which a fraction of nonmagnetic elements is substituted by magnetic transition-metal (TM) ions are ideal candidates. By interaction between the localized magnetic moments and band electrons or holes, it is possible to control magnetic order by means of carrier concentration.[1–4] The wide-band-gap zinc-oxide–based DMS's attract currently considerable attention. On the basis of a carrier Fermi sea interacting with localized spins, high Curie temperatures have been predicted for ZnO with Mn and hole doping.[5] Recent *ab initio* calculations predict that incorporation of V, Cr, Fe, Co, or Ni in ZnO in the 5–25% concentration range should give rise to metallic behavior and a ferromagnetic state without the need for additional doping.[6,7] The latter modeling, based on a partially occupied TM d band,[8] shows that the down spin $3d$ states of the TM ions enter the conduction band and that ferromagnetic double exchange interaction predominates. Electron doping should enhance this phenomenon.

Several experiments have been carried out in order to verify these predictions and to determine the Curie temperature T_C as a function of the nature of the TM ion, the TM concentration, and the carrier concentration. Ferromagnetic features, with T_C between 280 and 350 K, have been reported for Co (Refs. 9 and 10) and V (Ref. 11) -doped ZnO films, grown on α-Al_2O_3 substrates. The magnetic properties were shown to depend strongly on the carrier density (n-type), required to be in the range 10^{18}–10^{20} cm^{-3}.[9,11] The growth conditions (O_2 pressure and substrate temperature) as well as thermal annealing have also been found to influence the electron concentration, the magnetization, and the Curie temperature.[12,13] In particular, growth temperatures above 600 °C can produce inhomogeneous $Zn_{0.75}Co_{0.25}O$ films with ferromagnetic Co clusters and reduced electrical resistivity.

Presently, there is a lack of information on the sites occupied by the TM ions in the ZnO host, as well as on the magnetic state of these ions, since all experiments were based on the macroscopic magnetization of the films. It is of fundamental importance to determine the electronic state of the TM ions in a high concentration range in order to understand the interplay between carrier concentration and magnetic exchange coupling. The advantage of electron paramagnetic resonance (EPR) spectroscopy is its selectivity to the microscopic structure of the doping atom.

Epitaxial 1000-Å-thick (Zn,Co)O films with a nominal concentration [Co]=10% have been grown by pulsed laser deposition (PLD) on the $(000\bar{1})$ O face of semi-insulating ZnO substrates. Source materials were pressed ZnO and CoO targets. The composition and the crystalline quality of the layers have been characterized by Rutherford backscattering and x-ray diffraction.[14] The EPR measurements were performed with an X-band spectrometer operating in the 4–300-K temperature range. The absolute spin concentration has been determined by comparison with a calibrated ruby standard sample.

ZnO crystallizes in the wurtzite structure with a C_{3v} point symmetry. As with all $3d$ TM metals, Co is expected to substitute the Zn atoms; in its neutral charge state (as referred to the charge of the Zn ion), the Co_{Zn}^{2+} ion has an $[Ar]3d^7$ electron configuration. The atomic ^4F ground state splits under the influence of the tetrahedral component of the crystal field into a spin $S=\frac{3}{2}$ $^4A_2$ ground state and $^4T_2$ $+^4T_1$ excited states. The trigonal component of the crystal field (CF) and the spin-orbit interaction further splits the $^4A_2$ ground state into two Kramers doublets $E_{1/2}$, $E_{3/2}$ with a zero-field splitting equal to $2D$. The EPR data can be described by the following spin Hamiltonian:[15]

$$\mathcal{H}_s=\mu_B\mathbf{B}\cdot g\cdot\mathbf{S}+\mathbf{S}\cdot A\cdot\mathbf{I}+D[S_z^2-\tfrac{1}{3}S(S+1)], \qquad (1)$$

where μ_B is the Bohr magneton, **B** is the magnetic field, **S** and **I** are the electronic and the nuclear spin operators, respectively, and g and A are the Landé and hyperfine tensors, respectively. In the present case, $I=\frac{7}{2}$. The EPR parameters of the isolated substituting Co^{2+} cation in ZnO have only been reported briefly[16] and it is of interest to recall them here. Typical Co^{2+} EPR spectra observed in our nonintentionally doped substrates are shown in Fig. 1. The magnetic

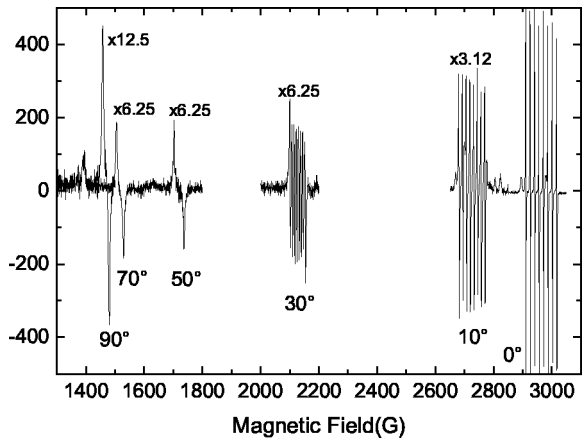

FIG. 1. EPR spectra of the isolated Co^{2+} ion for different orientations of the magnetic field relative to the crystal c axis.

field was applied in the $(2\bar{1}.0)_{ZnO}$ plane, the angle θ between **B** and the $[001]_{ZnO}$ axis being varied between 0° and 90°. The spin Hamiltonian $\mathcal{H}_s$ is written as

$$\mathcal{H}_s = \mu_B(g_\parallel B\cos\theta S_z + g_\perp B\sin\theta S_x) + A_\parallel S_z I_z + A_\perp(S_x I_x + S_y I_y) + D[S_z^2 - \tfrac{1}{3}S(S+1)], \quad (2)$$

where the labels z (or $\parallel$) and x (or $\perp$) apply for the directions $[001]_{ZnO}$ and $[120]_{ZnO}$, respectively. For **B** parallel to $[001]_{ZnO}$, the $\mathcal{H}_s$ matrix is diagonal and leads to the energies (excluding hyperfine terms which intervene to second order)

$$E = D(m_S^2 - 5/4) + g_\parallel \mu_B B m_S. \quad (3)$$

As the zero field splitting is high as compared to the microwave energy at the X band ($2D \gg h\nu$), only the transition between the lower $|m_S = -\frac{1}{2}\rangle$ and $|m_S = +\frac{1}{2}\rangle$ states are observed in the available magnetic field range 0–1 T. The hyperfine (HF) interaction gives rise to a characteristic octet structure ($\Delta E = g_\parallel \mu_B B + A_\parallel m_I$). For **B** parallel to $[120]_{ZnO}$, a mixing occurs between $E_{1/2}$ and $E_{3/2}$ states. Diagonalization of the $\mathcal{H}_s$ matrix leads to the energies

$$E = -(+)g_\perp \mu_B B/2 \pm [(g_\perp \mu_B B)^2 + D^2 + (-)g_\perp \mu_B B D]^{1/2}. \quad (4)$$

One observes in this case the transition between states separated by an energy $\Delta E = g_{\perp\,\mathrm{eff}}\mu_B B = 2g_\perp \mu_B B - \frac{3}{8}D\,(g_\perp \mu_B B/D)^3 \sim 2g_\perp \mu_B B$. Due to the small linewidth of ~1 G, the hyperfine interaction is well resolved for all angles. Numerical values of the derived EPR parameters are given in Table I. The EPR spectrum of the isolated Co^{2+} ion can be observed up to a temperature of 100 K and then disappears due to rapid line broadening. In the range 4–100 K, the EPR signal intensity varies according to the $(1/T)$ Curie law, as expected for isolated paramagnetic ions.

After growth of the 1000-Å-thick $Zn_{0.09}Co_{0.10}O$ layer, a new and different Co-related spectrum is observed (Fig. 2). The spectrum is characterized by an ~200-G large (peak-to-peak width) single line with effective g values ($g_{\parallel\,\mathrm{eff}}, g_{\perp\,\mathrm{eff}}$) close to but slightly different from those of the isolated Co^{2+} in the substrate (Table I). The shape of the Co^{2+} line from the layer is Lorentzian (in contrast to the single ion resonances, which have a Gaussian line shape), a fingerprint for the expected importance of exchange interaction between the Co^{2+} ions. The spin concentration has been obtained by a numerical double integration of the experimental spectrum for $B \perp c$ at $T = 4$ K. We find $[Co^{2+}] = 8\%$, a value close to the total Co concentration, which shows that PLD is a suitable growth technique to achieve high substitution rates while preserving the structure.

TABLE I. EPR parameters for the Co^{2+} ion in ZnO; the CF parameter is $D = 2.75\ \mathrm{cm}^{-1}$.

g factors	HF constant A (10^{-4} cm^{-1})	Linewidth ΔB_{pp} (G)	Reference
$g_\parallel = 2.243$	$A_\parallel = 16.11$		16
$g_\perp = 2.2791$	$A_\perp = 3.00$		
$g_\parallel = 2.2384$	$A_\parallel = 15.90$	$\Delta B_\parallel = 0.4$	ZnO:Co
$g_{\perp\,\mathrm{eff}} = 4.551$	$A_\perp = 2.90$	$\Delta B_\perp = 2.6$	substrate
$g_\perp = 2.2768$			This work
$g_\parallel = 2.2212$		$\Delta B_\parallel = 156$	$Zn_{0.9}Co_{0.1}O$
$g_{\perp\,\mathrm{eff}} = 4.5310$		$\Delta B_\perp = 200$	layer
$g_\perp = 2.2669$			This work

One may think the shift in the resonance field position of the new Co spectrum with respect to the isolated Co^{2+} octet is due to a change of the g values, as a consequence of the change of the crystal field (CF) in $Zn_{0.9}Co_{0.1}O$ with respect

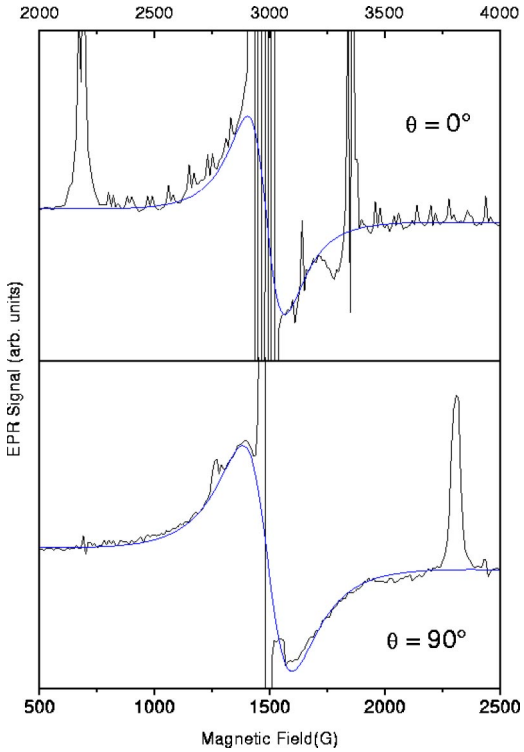

FIG. 2. (Color online) EPR spectra for the two principal orientations of the magnetic field ($\parallel, \perp c$). The total spectrum is a superposition of spectra from the substrate (Fe^{3+},Co^{2+},Ni^{3+}) and the Co^{2+} spectrum from the epitaxial layer.

to ZnO via the lattice constants. Actually, the CF acts negligibly on the $g_{\perp\,\mathrm{eff}}$ value alone [see Eqs. (3) and (4)]. The resonance shift is expected to be due essentially to the demagnetizing field related to magnetization induced by the high doping concentration. Assuming an assembly of isolated magnetic moments ($m_S g \mu_B$) governed by Boltzmann statistics, for a [Co^{2+}] concentration $N = 3.4 \times 10^{21}$ cm^{-3}, we derive from Eq. (3) a magnetization M at 4 K equal to 50 G for $\mathbf{B} \| \mathbf{c}$. We outline this value is between the values found neglecting the CF, that is, using $M = N g \mu_B S B_S[g \mu_B BS/(kT)]$, where B_S is the Brillouin function and $S = \frac{1}{2}$ or $\frac{3}{2}$. Also, the magnetization for $\mathbf{B} \perp \mathbf{c}$ is found reduced to 22 G [see Eq. (4)]. In the case of an isotropic g factor, the resonance condition is usually derived by minimizing the free-energy density,[17]

$$U = -\mu_o \mathbf{M} \cdot \mathbf{H}_{\mathrm{ext}} + \tfrac{1}{2} \mu_o \mathbf{M} \cdot N \cdot \mathbf{M}, \qquad (5)$$

where $\mathbf{H}_{\mathrm{ext}}$ is the external field, $\mathbf{M}$ is the saturation magnetization vector, and N is the demagnetizing tensor (for a thin film, $N_{xx} = N_{yy} = 0$, $N_{zz} = 1$). We assume this approach is still valid in the case of an anisotropic g factor given by $g = (g_\parallel^2 \cos^2\theta + g_{\perp\,\mathrm{eff}}^2 \sin^2\theta)^{1/2}$. The internal effective fields for $\theta = 0$ and $\pi/2$ are $H_{\mathrm{int}}(\perp \text{ plane}) = H_{\mathrm{ext}} - M$ and $H_{\mathrm{int}}(\text{in plane}) = [H_{\mathrm{ext}}(H_{\mathrm{ext}} + M)]^{1/2}$, respectively. The magnetization should shift the resonance field to a higher value for $\mathrm{H} \| c$ and to a lower value for $\mathrm{H} \perp c$. For $\mathrm{H} \| c$, we observe at 4 K a positive shift (+23 G) lower than that expected from a pure paramagnetic film (+50 G). This is an indication of antiferromagnetic coupling between the Co cations. For $\mathrm{H} \perp c$, the positive shift (+7 G) necessitates making intervening magnetocrystalline anisotropy. For a given magnitude of B, the ground state for $\mathbf{B} \perp \mathbf{c}$ is at lower energy than the ground state for $\mathbf{B} \| \mathbf{c}$ and the c axis should be the hard direction for magnetization. In our conditions ($B_\perp \sim B_\parallel/2$), the ground state for $\mathrm{B} \perp c$ has an energy very close to the one for $\mathrm{B} \| c$, and the anisotropy has an origin other than the crystal field. Phenomenological terms of the form ($-K \sin^2\theta$) must be added to Eq. (5) for deriving the true resonance condition. Defining the anisotropy field H_K by $K = \mu_o M H_K/2$, we evaluate the values at 4 K for $\mu_o M$ and $\mu_o H_k$ equal to 10 and 24 G, respectively.

Additional and more direct information about the paramagnetic or ferromagnetic or antiferromagnetic state of the layer can be obtained from the variation of the EPR spectrum intensity I with the temperature. In the case of cations without exchange interaction, the intensity I is proportional to the difference in population of the two lowest levels, whose energies are given by Eq. (3) for $\mathrm{B} \| c$ and by Eq. (4) for $\mathrm{B} \perp c$. The calculation gives a variation $I \sim (C/T)$ except in the region $T < 10$ K, where small deviations occur. The EPR spectrum for $\mathrm{B} \perp c$, which was the best resolved one, could be measured from 4 to 65 K. The results in the form (IT) versus T are shown in Fig. 3. Instead of a paramagnetic behavior, we observe a weak ferromagnetism with saturation near 4 K. To extract the Curie paramagnetic temperature Θ_p, we have replotted the results in Fig. 4 as I^{-1} versus T; extrapolation of the linear part gives $\Theta_p \sim +12$ K. The EPR spectrum for $\mathrm{B} \| c$ could only be measured up to 20 K. Interestingly, its

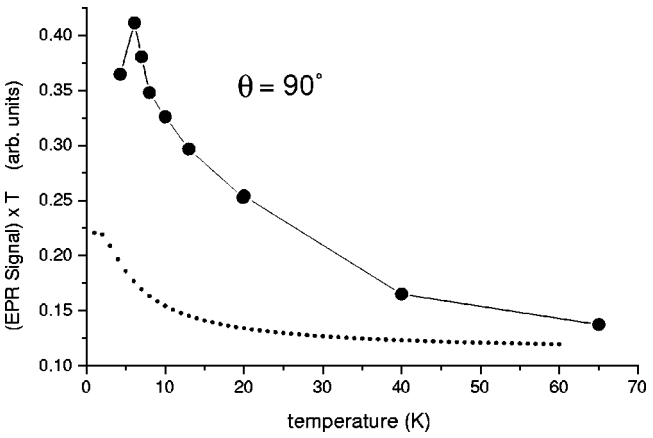

FIG. 3. EPR signal intensity times temperature vs temperature: experimental points for $\mathrm{H} \perp c$ and calculation (dotted line) for assembly of isolated Co^{2+} cations, taking into account CF splitting.

intensity decreases more rapidly with T than the spectrum for $\mathrm{B} \perp c$ (see the inset in Fig. 4). As already pointed out, though from the crystal field one expects the c axis to be the hard axis for magnetization, the EPR signal should not be sensitive to it. The anisotropy probably originates from anisotropic magnetic exchange interactions. Anisotropy has been evoked in an analysis of magnetic susceptibility from ZnO crystals with 0.049% of Co^{2+},[18] involving a small fraction of Co^{2+} ferromagnetic pairs. We rather think that moments order antiferromagnetic but nonparallel (canting), producing very weak ferromagnetism in accordance with the small value of Θ_p.

In the 10% concentration regime, a quantitative analysis of the EPR line shapes on the basis of clusters with different effective spins and orientations is not feasible. Dipolar interaction between identical spins $S = \frac{1}{2}$ should lead to a linewidth expressed in frequency units: $\Delta\omega$

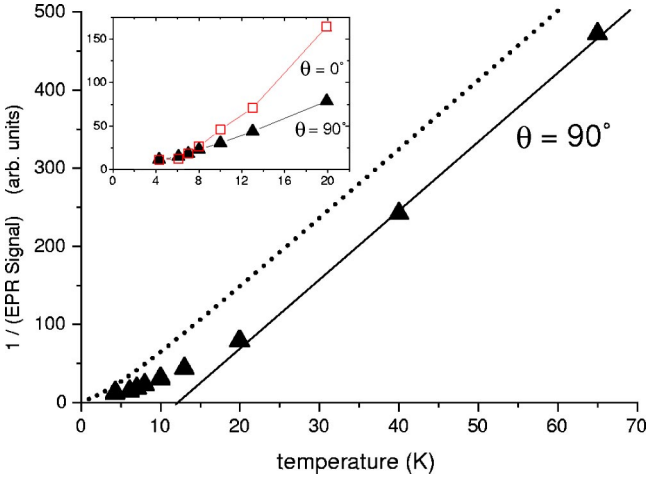

FIG. 4. (Color online) Inverse of the EPR signal intensity of the high concentration Co^{2+} line vs temperature for $\mathrm{H} \perp c$ (up triangles); the behavior expected from a pure paramagnetic film is given by the dotted line. The inset shows the low-temperature part for orientation $\mathrm{H} \| c$ (squares).

$=3.8(\mu_o/2\pi)\gamma^2\hbar N$, where $\gamma=g\mu_B/\hbar$ and N is the spin concentration. This gives 300 G for the peak-to-peak linewidth. The isotropic Heisenberg exchange interaction between cations of spins $\mathbf{S}_1$ and $\mathbf{S}_2$, of the form $(J_{12}\mathbf{S}_1\cdot\mathbf{S}_2)$, is known to induce narrowing and a Lorentzian shape. The anisotropic exchange may be expressed by terms of the form $\mathbf{D}_{12}\cdot(\mathbf{S}_1\times\mathbf{S}_2)$, where $\mathbf{D}_{12}$ is a constant vector.[19]

It should be noted that despite a careful search, no free-carrier-related EPR signal[20] could be observed in our layers. One may thus interpret the nonobservation of the ferromagnetic state by an insufficient free-carrier concentration. The possibility to mediate long-range ferromagnetic interactions by mean of carriers is an open question. Clearly one should obtain high carrier concentration to overcome the short-range antiferromagnetic coupling between Co^{2+} spins. As a matter of fact, ferromagnetic features with $T_C>280$ K have only been observed in samples with high electron concentrations $(3\times10^{20}\ \mathrm{cm}^{-3})$.[9] It has to be verified that the observed ferromagnetism did not arise from metallic Co clusters.

In conclusion, the EPR study of 10% Co-doped ZnO epitaxial layers has shown that, whereas the Co^{2+} ion is incorporated into the lattice (in substitution of Zn^{2+}), the free-carrier concentration stays low and no ferromagnetic ordering is observed. We give evidence of a paramagnetic behavior in the 20–65-K range with a critical temperature of $+12$ K for $B\perp c$. Nonvanishing antisymmetric spin coupling is suggested from the anisotropy observed in the 4–20-K range and the faint value of magnetization at 4 K.

*Electronic address: Nat.Jedrecy@lmcp.jessieu.fr

[1] H. Ohno, J. Magn. Magn. Mater. **110-129**, 200 (1999).
[2] S. J. Pearton *et al.*, J. Appl. Phys. **93**, 1 (2003).
[3] F. Matsukura, H. Ohno, A. Shen, and Y. Sugawara, Phys. Rev. B **57**, R2037 (1998).
[4] S. Koshihara *et al.*, Phys. Rev. Lett. **78**, 4617 (1997).
[5] T. Dietl, H. Ohno, F. Matsukura, J. Cibert, and D. Ferrand, Science **287**, 1019 (2000).
[6] K. Sato and H. Katayama-Yoshida, Jpn. J. Appl. Phys., Part 2 **39**, L555 (2000).
[7] H. Katayama-Yoshida, K. Sato, and T. Yamamoto, JSAP Int. **6**, 20 (2002).
[8] H. Akai, Phys. Rev. Lett. **81**, 3002 (1998).
[9] K. Ueda, H. Tabata, and T. Kawai, Appl. Phys. Lett. **79**, 988 (2001).
[10] H-J. Lee, S-Y. Jeong, C. R. Cho, and C. H. Park, Appl. Phys. Lett. **81**, 4020 (2002).
[11] H. Saeki, H. Tabata, and T. Kawai, Solid State Commun. **120**, 439 (2001).
[12] Y. M. Cho, W. K. Choo, H. Kim, D. Kim, and Y. E. Ihm, Appl. Phys. Lett. **80**, 3358 (2002).
[13] J. H. Kim, H. Kim, D. Kim, Y. E. Ihm, W. K. Choo, and M. Cho, J. Appl. Phys. **92**, 6066 (2002).
[14] Y. Zheng *et al.* (unpublished).
[15] A. Abragam and B. Bleaney, *Electron Paramagnetic Resonance of Transition Ions* (Clarendon, Oxford, 1970).
[16] T. Estle and M. De Wit, Bull. Am. Phys. Soc. **6**, 445 (1961).
[17] C. J. Oates, F. Y. Ogrin, S. L. Lee, P. C. Riedi, G. M. Smith, and T. Thomson, J. Appl. Phys. **91**, 1417 (2002); J. Smit and H. G. Beljers, Philips Res. Rep. **10**, 113 (1955).
[18] W. H. Brumage, C. F. Dorman, and C. R. Quade, Phys. Rev. B **63**, 104411 (2001).
[19] T. Moriya, Phys. Rev. **120**, 91 (1960).
[20] D. M. Hofmann, A. Hofstaetter, F. Leiter, H. Zhou, F. Henecker, B. Meyer, S. B. Orlinskii, I. Schmidt, and P. G. Baranov, Phys. Rev. Lett. **88**, 045504 (2002).